

# Manganese(III) Salen Complex Immobilized on $\text{Fe}_3\text{O}_4$ Magnetic Nanoparticles: The Efficient, Green and Reusable Nanocatalyst

Seyed Mohsen Sadeghzadeh,<sup>\*a</sup> Faeze Daneshfar,<sup>b</sup> and Maryam Malekzadeh<sup>c</sup>

<sup>a</sup>Department of Chemistry, College of Sciences, Birjand University, P.O. Box 97175-615, Birjand, Iran

<sup>b</sup>Department of Physics, College of Sciences, Birjand University, P.O. Box 97175-614, Birjand, Iran

<sup>c</sup>Department of Chemistry, Payame Noor University, Tabas, Iran

A new  $\text{Fe}_3\text{O}_4$  magnetic nanoparticles supported manganese salen complex was successfully prepared by attaching manganese acetates to a novel *N,N'*-bis(salicylidine)ethylenediamine ligand functionalized  $\text{Fe}_3\text{O}_4$ . The as-prepared catalyst was characterized by TGA, XRD, FTIR, VSM, and TEM. It was found to be an efficient catalyst for the synthesis of benzopyranopyrimidines in aqueous medium. High catalytic activity and ease of recovery from the reaction mixture using external magnet, and several reuse times without significant losses in performance are additional eco-friendly attributes of this catalytic system.

**Keywords** salen, nanocatalyst, benzopyranopyrimidine, green chemistry, solvent free

## Introduction

Currently one of the most important synthetic ligand systems, especially in the context of asymmetric catalysis, are the tetradentate Schiff bases known as salen (*N,N'*-bis(salicylaldehydo)ethylenediamine). In 1889, while studying the effect of diamines on diketones, Combes prepared the first salen ligand and its Cu complex.<sup>[1]</sup> Since then, salen derivatives and their metal complexes have been synthesised and characterized and gradually their value as catalysts has become recognised.<sup>[2]</sup> With the growth in interest in enantiomerically pure compounds for the pharmaceutical and agrochemical industries, it is perhaps not surprising that in the last decade attention has focused on chiral salen ligands, and in particular on the use of their optically pure metal complexes as asymmetric catalysts. Applications have grown rapidly and a broad range of asymmetric catalyses have now been described including oxidations, additions and reductions.

In recent years, core–shell multi-components have attracted intense attention because of their potential applications in catalysis.<sup>[3]</sup> Different from single-component that can only supply people with one function, the core–shell multi-components can integrate multiple functions into one system for specific applications.<sup>[4–8]</sup> Moreover, the interactions between different components can greatly improve the performance of the multi-components system and even generate new synergistic

properties. Among the core–shell structured composites, the composites with magnetic core and functional shell structures have received especial attention because of their potential applications in catalysis, drug storage/release, selective separation, chromatography, and chemical or biologic sensors.<sup>[9–15]</sup> The magnetic core has good magnetic responsibility, and can be easily magnetized. Therefore, the composites with magnetic core can be conveniently collected, separated or fixed by external magnet.

Control of selectivity, for example, chemo- and regioselectivity, is among the most important objectives in organic chemistry. For multicomponent reactions involving the simultaneous molecular interaction of three or more components, the issue of selectivity is of particular significance due to the high probability of several potential parallel reaction pathways leading to different product classes.<sup>[16–18]</sup> Many different process parameters such as temperature, pressure, solvent, catalyst type, as well as kinetic or thermodynamic control, and other factors can be utilized to modulate the selectivity of synthetic transformations.<sup>[19–24]</sup> In addition to these classical reaction parameters, the use of microwave irradiation<sup>[25–28]</sup> or sonication<sup>[29–31]</sup> has provided additional opportunities to execute reactions and to tune selectivities in organic synthesis. A challenging example in this context is multicomponent condensation reactions of 2-hydroxybenzaldehyde (**1**), malononitrile (**2**), and amine (**3**) which in general can lead to the formation of

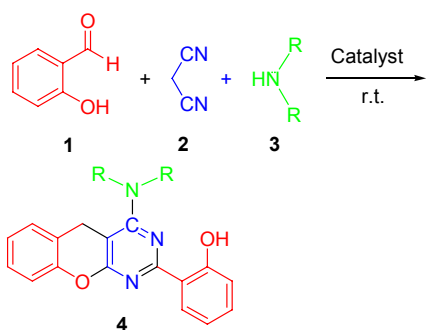
\* E-mail: sadeghzadeh\_sm@yahoo.com; Tel.: 0098-561-2502065; Fax: 0098-561-2502065

Received January 1, 2014; accepted February 9, 2014; published online XXXXX, 2014.

Supporting information for this article is available on the WWW under <http://dx.doi.org/10.1002/cjoc.201400007> or from the author.

several different tricyclic reaction products (Scheme 1) due to the presence of at least three nonequivalent nucleophilic reaction centers in the benzopyranopyrimidines building block **4**. Engaged in the development of greener and sustainable pathways for organic transformations, nanomaterial, and nano-catalysis,<sup>[32–35]</sup> herein, we report a simple and efficient synthesis of a nano-ferrite-supported, magnetically recyclable, and inexpensive manganese(III) catalyst and its application for the synthesis of benzopyranopyrimidines.

**Scheme 1** Synthesis of benzopyranopyrimidines from salicylic aldehydes, malononitrile, and amine in the presence of  $\text{Fe}_3\text{O}_4\backslash\text{SiO}_2\backslash\text{Salen}\backslash\text{Mn}$  MNPs



## Experimental

### Materials and methods

Chemical materials were purchased from Fluka and Merck in high purity. Melting points were determined in open capillaries using an Electrothermal 9100 apparatus and are uncorrected. FTIR spectra were recorded on a VERTEX 70 spectrometer (Bruker) in the transmission mode in spectroscopic grade KBr pellets for all the powders. The particle size and structure were observed by using a Philips CM10 transmission electron microscope operating at 100 kV. Powder X-ray diffraction data were obtained using Bruker D8 Advance model with Cu K $\alpha$  radiation. The thermogravimetric analysis (TGA) was carried out on a NETZSCH STA449F3 at a heating rate of  $10\ ^\circ\text{C}\cdot\text{min}^{-1}$  under nitrogen. The magnetic measurement was carried out in a vibrating sample magnetometer (VSM) (4 inch, Daghighe Meghnatis Kashan Co., Kashan, Iran) at room temperature. NMR spectra were recorded in  $\text{CDCl}_3$  on a Bruker Avance DRX-400 MHz instrument spectrometer using TMS as internal standard. The purity determination of the products and reaction monitoring were accomplished by TLC on silica gel polygram SILG/UV 254 plates.

### General procedure for the preparation of $\text{Fe}_3\text{O}_4$ nanoparticles

The synthesis procedure for the preparation of  $\text{Fe}_3\text{O}_4$  nanoparticles is illustrated as follows: (1) 0.01 mol  $\text{FeCl}_2\cdot 4\text{H}_2\text{O}$  and 0.03 mol  $\text{FeCl}_3\cdot 6\text{H}_2\text{O}$  were dissolved in 200 mL distilled water, followed by the addition of PEG (1.0 g, MW 6000). (2) Sodium hydroxide (NaOH) was added to the solution and the pH value was con-

trolled in the range  $12 \leq \text{pH} \leq 13$ . (3) Different amount of hydrazine hydrate ( $\text{N}_2\text{H}_4\cdot\text{H}_2\text{O}$ , 80% concentration) was added to the above suspension. The reaction was continued for about 24 h at room temperature. During this period, the pH value was adjusted by NaOH and kept in the range  $12 \leq \text{pH} \leq 13$ . The black  $\text{Fe}_3\text{O}_4$  NPs were then rinsed several times with ionized water.

### General procedure for the preparation of $\text{Fe}_3\text{O}_4\backslash\text{SiO}_2$ nanoparticles

0.02 mol of  $\text{Fe}_3\text{O}_4$  MNP was dispersed in a mixture of 80 mL of ethanol, 20 mL of deionized water and 2.0 mL of 28 wt% concentrated ammonia aqueous solution ( $\text{NH}_3\cdot\text{H}_2\text{O}$ ), followed by the addition of 0.20 g of tetraethyl orthosilicate (TEOS). After vigorous stirring for 24 h, the final suspension was repeatedly washed, filtered for several times and dried at  $60\ ^\circ\text{C}$  in the air.

### General procedure for the preparation of compound (A) nanoparticles

For synthesis of compound (A) MNP, 2 mmol of  $\text{Fe}_3\text{O}_4\backslash\text{SiO}_2$  MNPs were dispersed in a mixture of 80 mL of ethanol, 20 mL of deionized water and 2.0 mL of 28 wt% concentrated ammonia aqueous solution ( $\text{NH}_3\cdot\text{H}_2\text{O}$ ), followed by the addition of 20 mmol of ethyl 3,4-diaminobenzoate. After vigorous stirring for 24 h, the magnetic  $\text{Fe}_3\text{O}_4\backslash\text{SiO}_2$  nanoparticles were collected by magnetic separation and washed with ethanol and deionized water in sequence.

### General procedure for the preparation of $\text{Fe}_3\text{O}_4\backslash\text{SiO}_2\backslash\text{Salen}$ ( $N,N'$ -bis(salicylidine)ethylenediamine) nanoparticles

For synthesis of  $\text{Fe}_3\text{O}_4\backslash\text{SiO}_2\backslash\text{Salen}$  MNPs, compound (A) (4 g) was suspended in 600 mL of  $0.1\ \text{mol}\cdot\text{L}^{-1}$  toluene solution of salicylaldehyde and the colloidal solution was refluxed for 24 h. The magnetic  $\text{Fe}_3\text{O}_4\backslash\text{SiO}_2\backslash\text{Salen}$  nanoparticles were collected by magnetic separation and washed with ethanol and deionized water in sequence.

### General procedure for the preparation of $\text{Fe}_3\text{O}_4\backslash\text{SiO}_2\backslash\text{Salen}\backslash\text{Mn}$ nanoparticles

$\text{Fe}_3\text{O}_4\backslash\text{SiO}_2\backslash\text{Salen}$  (0.45 g) was added to an excess of pyridine dissolved in dichloromethane/ionic liquid, to which  $\text{Mn}(\text{OAc})_2$  (0.65 g) was subsequently added. pH was maintained at 9 by addition of sodium borohydride. The reaction mixture was kept under magnetic stirring overnight. The final particle was separated from the solution by applying a magnetic field, washed three times with water to remove any ions present, and dried under vacuum.<sup>[36]</sup>

### General procedure for the synthesis of benzopyranopyrimidines

2-Hydroxybenzaldehyde (2 mmol), malononitrile (1 mmol), amine (1 mmol) and  $\text{Fe}_3\text{O}_4\backslash\text{SiO}_2\backslash\text{Salen}\backslash\text{Mn}$  MNPs (0.0008 g) were stirred at room temperature under solvent-free conditions for the appropriate time.

Upon completion, the progress of the reaction was monitored by TLC. When the reaction was completed, EtOH was added to the reaction mixture and the  $\text{Fe}_3\text{O}_4$ \SiO<sub>2</sub>\Salen\Mn MNPs was separated by external magnet. Then the solvent was removed from solution under reduced pressure and the resulting product was purified by recrystallization using ethanol.

## Results and Discussion

The first step in the accomplishment of this goal was the synthesis and functionalization of magnetic nanoparticles (Figure 1). The catalyst was prepared by sonicating nano-ferrites with salen [which acts as a robust anchor and avoids Mn(III)] in absolute MeOH, followed by addition of Mn(OAc)<sub>2</sub>. Material with Mn(III) on the functionalized nano-ferrites was obtained in excellent yield. The synthesized  $\text{Fe}_3\text{O}_4$ \SiO<sub>2</sub>\Salen\Mn MNP was then characterized by different methods such as XRD, TEM, VSM, FTIR and TGA.

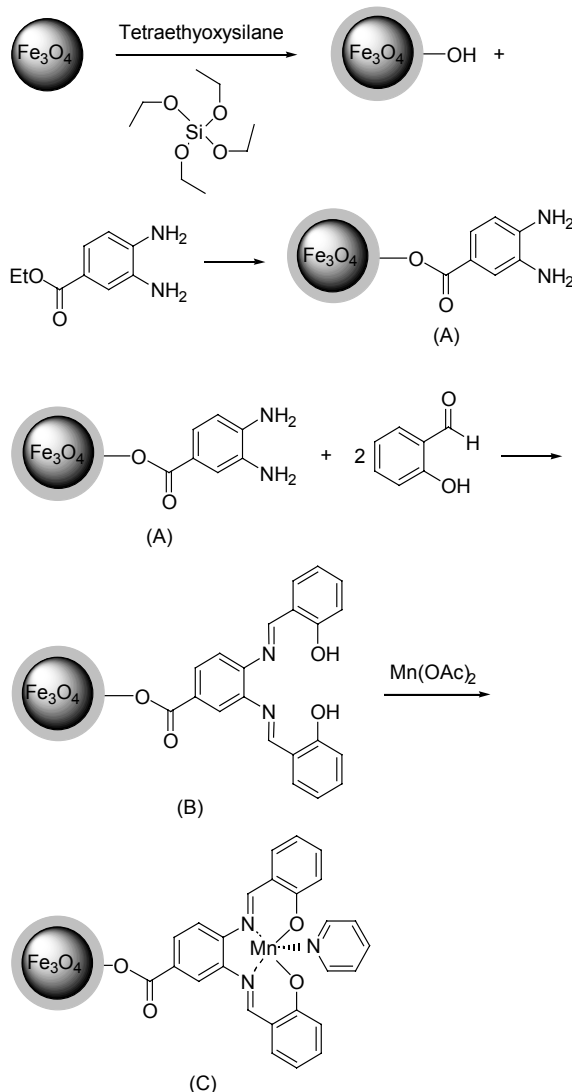


**Figure 1** Schematic illustration of the synthesis for  $\text{Fe}_3\text{O}_4$ \SiO<sub>2</sub>\Salen\Mn nanoparticles.

The structural properties of synthesized  $\text{Fe}_3\text{O}_4$ \SiO<sub>2</sub>\Salen\Mn MNP were analyzed by X-ray power diffraction (XRD). As shown in Figure 2, XRD patterns of the synthesized  $\text{Fe}_3\text{O}_4$ \SiO<sub>2</sub>\Salen\Mn nanoparticle display several relatively strong reflection peaks in the  $2\theta$  region of  $20^\circ$ – $70^\circ$ , which is quite similar to those of  $\text{Fe}_3\text{O}_4$  nanoparticles reported by other groups. The discernible six diffraction peaks in Figure 2a can be indexed to (220), (311), (400), (422), (511), and (440) which match well with the database of magnetite in JCPDS (JCPDS card No. 19-0629) file. Besides the peak of iron oxide, the XRD pattern of  $\text{Fe}_3\text{O}_4$ \SiO<sub>2</sub> core-shell nanoparticles presented a broad featureless XRD peak at low diffraction angle, which corresponded to the amorphous state SiO<sub>2</sub> shells (Figure 2b) (JCPDS card No. 29-0085). Figure 2c shows a typical XRD pattern of the  $\text{Fe}_3\text{O}_4$ \SiO<sub>2</sub>\Salen\Mn MNP.

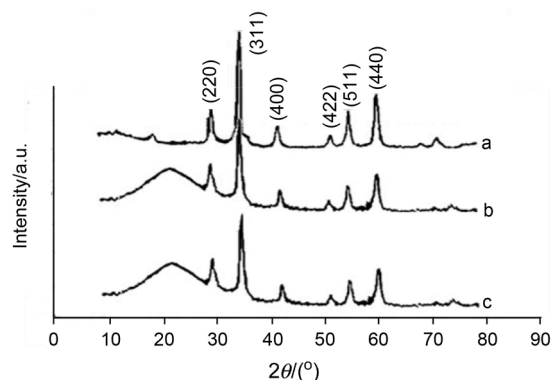


**Figure 2** XRD analysis of (a)  $\text{Fe}_3\text{O}_4$ , (b)  $\text{Fe}_3\text{O}_4$ \SiO<sub>2</sub>, and (c)  $\text{Fe}_3\text{O}_4$ \SiO<sub>2</sub>\Salen\Mn.

The successful synthesis of the  $\text{Fe}_3\text{O}_4$ \SiO<sub>2</sub>\Salen\Mn nanoparticles was confirmed by the FTIR spectra (Figure 3). The peaks at  $3415\text{ cm}^{-1}$  and  $590\text{ cm}^{-1}$  appear in all the FTIR spectra, which are assigned to the  $-\text{OH}$  group and the Fe—O group, respectively (Figure 3a). In FTIR spectra of the  $\text{Fe}_3\text{O}_4$ \SiO<sub>2</sub> MNPs, the absorption intensity of Fe—O group decreases with the addition of silica portion and a strong absorption intensity of the Si—O—Si group appears at  $1090\text{ cm}^{-1}$  owing to the silica coat (Figure 3b). Peaks appeared at  $3120$ ,  $2930$ ,  $1720$ , and  $1610\text{ cm}^{-1}$  are due to the stretching of the C—H aromatic group, the C—H aliphatic group, C=O group, and C=N group in the  $\text{Fe}_3\text{O}_4$ \SiO<sub>2</sub>\Salen\Mn MNP, respectively (Figure 3c).

The size and structure of the  $\text{Fe}_3\text{O}_4$ \SiO<sub>2</sub>\Salen\Mn MNP were also evaluated using transmission electron microscopy (TEM) (Figure 4). The average size of  $\text{Fe}_3\text{O}_4$  MNPs is about 15–20 nm (Figure 4a). After being coated with a silica layer, the typical core-shell structure of the  $\text{Fe}_3\text{O}_4$ \SiO<sub>2</sub> MNPs can be observed. The dispersity of  $\text{Fe}_3\text{O}_4$ \SiO<sub>2</sub> MNPs is also improved, and the average size increases to about 20–25 nm (Figure 4b). The TEM image of the  $\text{Fe}_3\text{O}_4$ \SiO<sub>2</sub>\Salen\Mn MNPs is shown in Figure 4c. The functionalization of

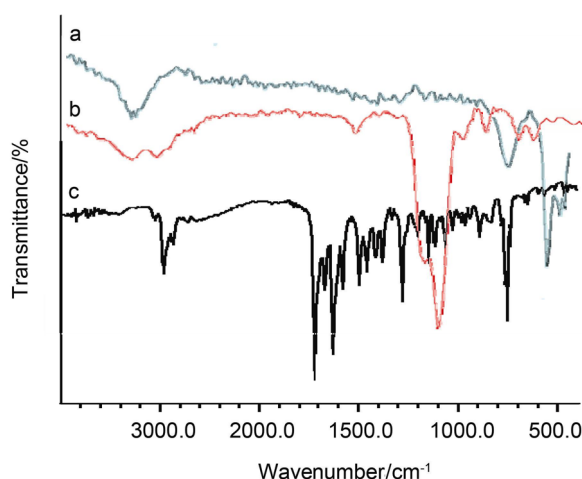


**Figure 3** FTIR spectra of (a)  $\text{Fe}_3\text{O}_4$ , (b)  $\text{Fe}_3\text{O}_4\backslash\text{SiO}_2$ , (c)  $\text{Fe}_3\text{O}_4\backslash\text{SiO}_2\backslash\text{Salen}\backslash\text{Mn}$ .

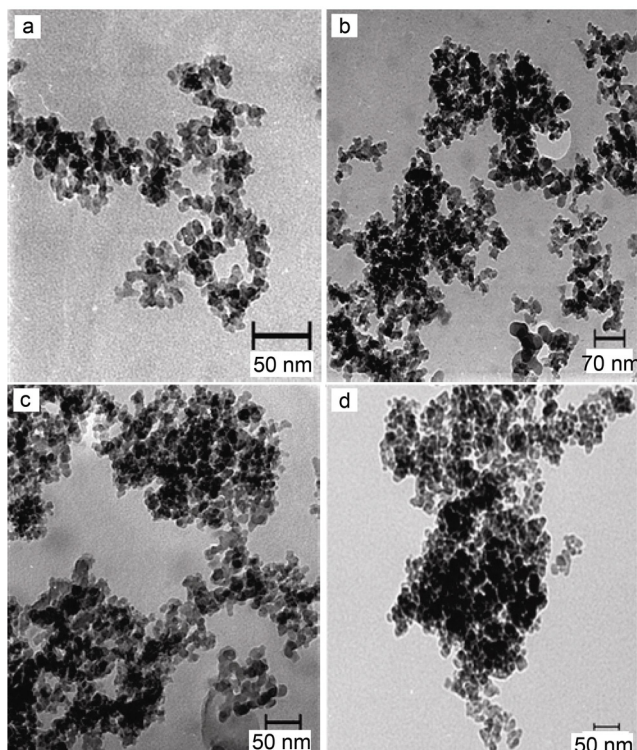


**Figure 4** TEM images of (a)  $\text{Fe}_3\text{O}_4$  MNPs, (b)  $\text{Fe}_3\text{O}_4\backslash\text{SiO}_2$  MNPs, (c)  $\text{Fe}_3\text{O}_4\backslash\text{SiO}_2\backslash\text{Salen}\backslash\text{Mn}$  MNPs, and (d)  $\text{Fe}_3\text{O}_4\backslash\text{SiO}_2\backslash\text{Salen}\backslash\text{Mn}$  MNPs after seven reuses.

the  $\text{Fe}_3\text{O}_4\backslash\text{SiO}_2\backslash\text{Salen}\backslash\text{Mn}$  MNPs does not result in the change of the morphology and size of the obtained  $\text{Fe}_3\text{O}_4\backslash\text{SiO}_2$  MNPs. The thermal behavior of  $\text{Fe}_3\text{O}_4\backslash\text{SiO}_2\backslash\text{Salen}\backslash\text{Mn}$  MNP is shown in Figure 5a. A significant decrease in the weight percentage of the  $\text{Fe}_3\text{O}_4\backslash\text{SiO}_2\backslash\text{Salen}\backslash\text{Mn}$  MNP at about 130 °C is related to desorption of water molecules from the catalyst surface. This was evaluated to be 1%–3% according to the TG analysis. In addition, the analysis showed two other decreasing peaks. The first peak appears at temperature around 250–280 °C due to the decomposition of Mn. This is fol-

lowed by a second peak at 420–460 °C, corresponding to the loss of the organic spacer group.

The magnetic properties of the nanoparticles were characterized using a vibrating sample magnetometer (VSM). The magnetization curves of the obtained nanocomposite registered at 300 K show that nearly no residual magnetism is detected (Figure 5b), which means that the nanocomposite exhibited the paramagnetic characteristics. Magnetic measurement shows that pure  $\text{Fe}_3\text{O}_4$ , and  $\text{Fe}_3\text{O}_4\backslash\text{SiO}_2\backslash\text{Salen}\backslash\text{Mn}$  MNPs have saturation magnetization values of 60.2, and 33.2 emu/g respectively. These nanocomposites with paramagnetic characteristics and high magnetization values can quickly respond to the external magnetic field and quickly redisperse once the external magnetic field is removed. The result reveals that the nanocomposites exhibit good magnetic responsibility, which suggests a potential application for targeting and separation.

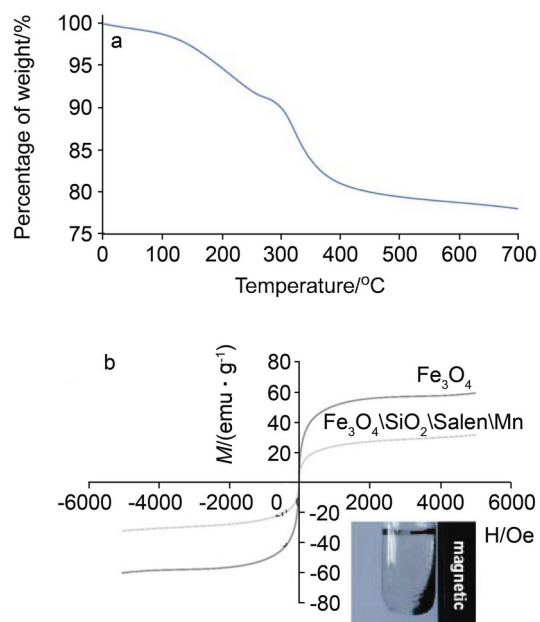


**Figure 5** (a) TGA diagram of nano catalysis; (b) Room-temperature magnetization curves of the nano catalysis.

The catalytic potential of the  $\text{Fe}_3\text{O}_4\backslash\text{SiO}_2\backslash\text{Salen}\backslash\text{Mn}$  MNPs was evaluated in condensation reactions. At first, the reaction of salicylic aldehydes, diethyl amine, and malononitrile was chosen as a model reaction to optimize the reaction conditions such as the amount of the catalyst, temperature, time, and solvent (Table 1). It was found that the best yield of the product was obtained at room temperature under solvent-free conditions in the presence of 0.0008 g of  $\text{Fe}_3\text{O}_4\backslash\text{SiO}_2\backslash\text{Salen}\backslash\text{Mn}$  MNPs for 50 min (Table 1, Entry 13). Three separated reactions were examined in the absence of any catalyst and in the presence of  $\text{Fe}_3\text{O}_4$  and  $\text{Fe}_3\text{O}_4\backslash\text{SiO}_2\backslash\text{Salen}$  MNPs. The results of these studies showed that any amount of the desired product was not formed (Table 1, Entries 15–17). A similar reaction in the presence of  $\text{Mn}(\text{OAc})_2$  as a

**Table 1** Optimization of the reaction conditions for the synthesis of benzopyranopyrimidine in terms of temperature, catalyst amount, time and product yield

Entry	Catalyst	Solvent	Temp./°C	Time/min	Catalyst amount/g	Yield <sup>a</sup> /%
1	Fe <sub>3</sub> O <sub>4</sub> \SiO <sub>2</sub> \Salen\Mn	—	r.t.	70	0.001	96
2	Fe <sub>3</sub> O <sub>4</sub> \SiO <sub>2</sub> \Salen\Mn	H <sub>2</sub> O	r.t.	70	0.001	23
3	Fe <sub>3</sub> O <sub>4</sub> \SiO <sub>2</sub> \Salen\Mn	EtOH	r.t.	70	0.001	48
4	Fe <sub>3</sub> O <sub>4</sub> \SiO <sub>2</sub> \Salen\Mn	THF	r.t.	70	0.001	37
5	Fe <sub>3</sub> O <sub>4</sub> \SiO <sub>2</sub> \Salen\Mn	CH <sub>2</sub> Cl <sub>2</sub>	r.t.	70	0.001	24
6	Fe <sub>3</sub> O <sub>4</sub> \SiO <sub>2</sub> \Salen\Mn	n-Hexane	r.t.	70	0.001	14
7	Fe <sub>3</sub> O <sub>4</sub> \SiO <sub>2</sub> \Salen\Mn	—	80	70	0.001	96
8	Fe <sub>3</sub> O <sub>4</sub> \SiO <sub>2</sub> \Salen\Mn	—	90	70	0.001	96
9	Fe <sub>3</sub> O <sub>4</sub> \SiO <sub>2</sub> \Salen\Mn	—	100	70	0.001	96
10	Fe <sub>3</sub> O <sub>4</sub> \SiO <sub>2</sub> \Salen\Mn	—	r.t.	60	0.001	96
11	Fe <sub>3</sub> O <sub>4</sub> \SiO <sub>2</sub> \Salen\Mn	—	r.t.	50	0.001	96
12	Fe <sub>3</sub> O <sub>4</sub> \SiO <sub>2</sub> \Salen\Mn	—	r.t.	40	0.001	73
13	Fe <sub>3</sub> O <sub>4</sub> \SiO <sub>2</sub> \Salen\Mn	—	r.t.	50	0.0008	96
14	Fe <sub>3</sub> O <sub>4</sub> \SiO <sub>2</sub> \Salen\Mn	—	r.t.	50	0.0006	75
15	—	—	r.t.	50	0.0008	—
16	Fe <sub>3</sub> O <sub>4</sub>	—	r.t.	50	0.0008	—
17	Fe <sub>3</sub> O <sub>4</sub> \SiO <sub>2</sub> \Salen	—	r.t.	50	0.0008	—
18	Mn(OAc) <sub>2</sub>	—	r.t.	50	0.0008	69

<sup>a</sup> Isolated yields.

non-supported catalyst gave the desired product in moderate yield (69%) due to the formation of by-products (Table 1, Entry 18). This result indicated that the catalytic efficiency of Mn(OAc)<sub>2</sub> was increased by immobilization onto Fe<sub>3</sub>O<sub>4</sub>.

The catalytic activity of the Fe<sub>3</sub>O<sub>4</sub>\SiO<sub>2</sub>\Salen\Mn MNPs was compared with that of the Salen\Mn. For this purpose, the reactions were carried out separately at room-temperature under solvent-free conditions with both the catalysts for the appropriate time (Table 2). The aliquots of the reaction mixture were collected periodically at an interval of 10 min. Table 2 shows the variation of the yields of benzopyranopyrimidine with time, when Fe<sub>3</sub>O<sub>4</sub>\SiO<sub>2</sub>\Salen\Mn MNPs and Salen\Mn were employed as catalysts. It is evident that, the catalytic activity of the Fe<sub>3</sub>O<sub>4</sub>\SiO<sub>2</sub>\Salen\Mn MNPs is similar to the Salen\Mn. After 50 min, Fe<sub>3</sub>O<sub>4</sub>\SiO<sub>2</sub>\Salen\Mn MNPs showed 96% preparation of benzopyranopyrimidine as compared to 91% with Salen\Mn. After 70 min, yield of the product in the presence of Fe<sub>3</sub>O<sub>4</sub>\SiO<sub>2</sub>\Salen\Mn MNPs is fixed at 96%, but Salen\Mn MNPs showed 98% preparation of benzopyranopyrimidine. The nano-sized particles increase the exposed surface area of the active component of the catalyst, thereby enhancing the contact between reactants and catalyst dramatically and mimicking the homogeneous catalysts. Also, the activity and selectivity of nano-catalyst can be manipulated by tailoring chemical and physical properties like size, shape, composition and morphology.

After optimization of the reaction conditions, to delineate this approach, particularly in regard to library

**Table 2** Comparison of the catalytic activity of Fe<sub>3</sub>O<sub>4</sub>\SiO<sub>2</sub>\Salen\Mn MNPs with that of Salen\Mn

Entry	Reaction time/min	Yield <sup>a</sup> /%	
		Fe <sub>3</sub> O <sub>4</sub> \SiO <sub>2</sub> \Salen\Mn	Salen\Mn
1	30	67	64
2	40	73	71
3	50	96	91
4	60	96	95
5	70	96	98

<sup>a</sup> Isolated yields.

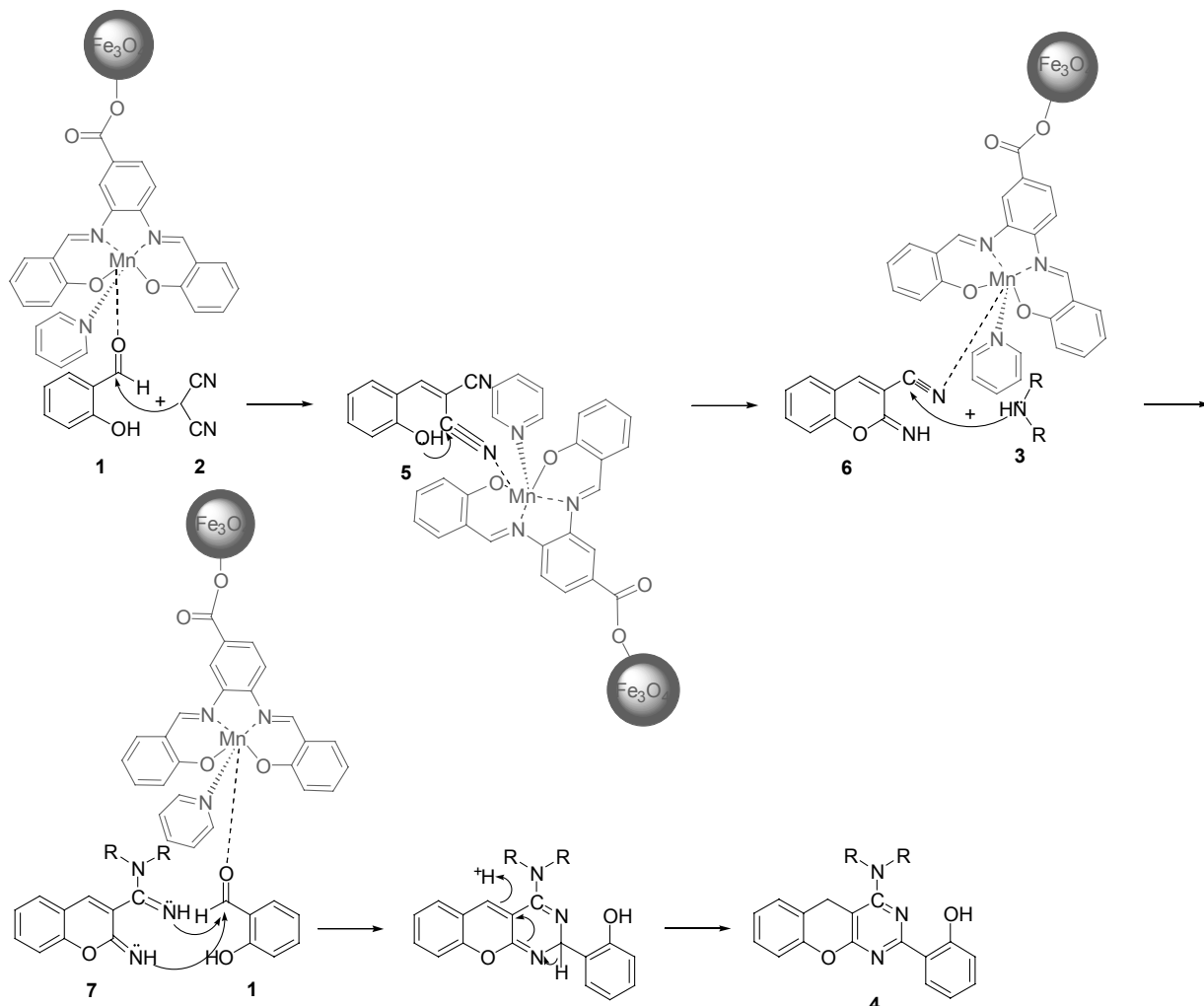
construction, this methodology was evaluated by using different amines, variety of different substituted 2-hydroxybenzaldehyde and of malononitrile in the presence of Fe<sub>3</sub>O<sub>4</sub>\SiO<sub>2</sub>\Salen\Mn MNPs under similar conditions. As can be seen from Table 3, electronic effects and the nature of substituents on the amines and 2-hydroxybenzaldehyde did not show strongly obvious effects in terms of yields under the reaction conditions. The four-component cyclocondensation reaction proceeded smoothly. High yields and excellent TONs and TOFs were achieved in all the cases.

Mechanistically, the reaction occurs via initial formation of arylidene malononitrile **5** by the Knoevenagel condensation between **1** and **2** followed by subsequent Pinner reaction (**5**→**6**). Next, the cyano group of intermediate **6** can be attacked by the amine **3** to produce intermediate **7**. Finally, amine **7** reacts with another molecule of salicylic aldehyde **1** followed by proton transfer to afford the product **4** (Scheme 2).

**Table 3** Synthesis of benzopyranopyrimidines derivatives catalyzed by  $\text{Fe}_3\text{O}_4\text{\textbackslash SiO}_2\text{\textbackslash Salen\textbackslash Mn MNPs}^a$ 

Entry	Aldehyde	Amine	Product	Yield <sup>b</sup> /%	TON	TOF/h <sup>-1</sup>	Entry	Aldehyde	Amine	Product	Yield <sup>b</sup> /%	TON	TOF/h
1			<b>4a</b>	96 <sup>[37]</sup>	$96 \times 10^4$	$115 \times 10^4$	5			<b>4e</b>	93 <sup>[37]</sup>	$93 \times 10^4$	$112 \times 10^4$
2			<b>4b</b>	95 <sup>[37]</sup>	$95 \times 10^4$	$114 \times 10^4$	6			<b>4f</b>	94 <sup>[37]</sup>	$94 \times 10^4$	$113 \times 10^4$
3			<b>4c</b>	82 <sup>[37]</sup>	$82 \times 10^4$	$98 \times 10^4$	7			<b>4g</b>	95 <sup>[37]</sup>	$95 \times 10^4$	$114 \times 10^4$
4			<b>4d</b>	95	$95 \times 10^4$	$114 \times 10^4$							

<sup>a</sup> Reaction condition: 2-hydroxybenzaldehyde (2 mmol), malononitrile (1 mmol), amine (1 mmol) and  $\text{Fe}_3\text{O}_4\text{\textbackslash SiO}_2\text{\textbackslash Salen\textbackslash Mn MNPs}$  (0.0008 g) at room-temperature. <sup>b</sup> Yield refers to isolated product.

**Scheme 2** A possible mechanism for the one-pot reaction for synthesis of benzopyranopyrimidines

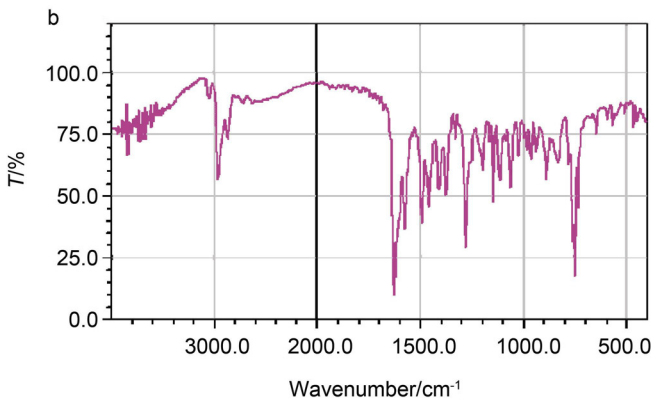
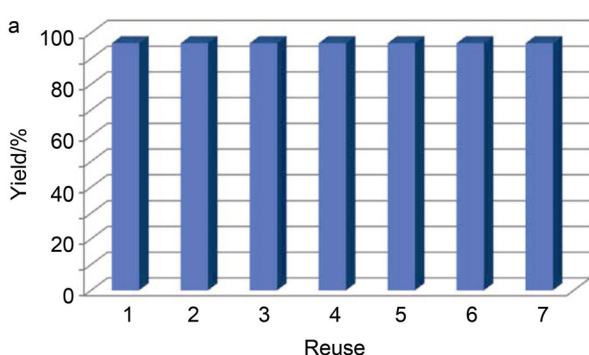


**Figure 6** (a) Reuses performance of the catalysts; (b) FT-IR spectrum of recovered Fe<sub>3</sub>O<sub>4</sub>\SiO<sub>2</sub>\Salen\{Mn MNPs.

It is important to note that the magnetic property of Fe<sub>3</sub>O<sub>4</sub>\SiO<sub>2</sub>\Salen\{Mn MNPs facilitates its efficient recovery from the reaction mixture during work-up procedure. The activity of the recycled catalyst was also examined under the optimized conditions. After the completion of reaction, the catalyst was separated by an external magnet, washed with methanol and dried at the pump. The recovered catalyst was reused for seven consecutive cycles without any significant loss in catalytic activity (Figure 6a).

The recyclability test was stopped after seven runs. Comparison of TEM images (Figure 4d) and FT-IR spectra of used catalyst (Figure 6b) with those of the fresh catalyst (Figure 3 and 4a) showed that the morphology and structure of Fe<sub>3</sub>O<sub>4</sub>\SiO<sub>2</sub>\Salen\{Mn MNPs remained intact after seven recoveries.

## Conclusions

In summary, Fe<sub>3</sub>O<sub>4</sub>\SiO<sub>2</sub>\Salen\{Mn MNP as a new magnetic nanoparticles catalyst was synthesized directly through reaction of Mn(OAc)<sub>2</sub> complex supported on Fe<sub>3</sub>O<sub>4</sub>\SiO<sub>2</sub>\Salen MNP. The synthesized Fe<sub>3</sub>O<sub>4</sub>\SiO<sub>2</sub>\Salen\{Mn MNP was used as a magnetically recyclable heterogeneous catalyst for the efficient one-pot synthesis of benzopyranopyrimidines from the reaction of 2-hydroxybenzaldehyde, malononitrile, and amine with high product yields. The catalytic research on novel approaches toward nanomaterials should be improved to enhance organic synthesis. For that purpose, nanoparticles catalyst provides a new way for continuous processes, because of its simple recyclability. From a scientific point, our results expand the application of nanoparticles. This catalyst should be helpful to the development of new catalytic systems.

## References

- [1] Combes, A. C. R. Acad. Fr. **1889**, *108*, 1252.
- [2] Sheldon, R. A.; Kochi, J. K. In *Metal Catalysed Oxidations of Organic Compounds*, Academic Press, New York, **1981**, pp. 97, 102 and 105.
- [3] Zhu, C. L.; Zhang, M. L.; Qiao, Y. J.; Xiao, G.; Zhang, F.; Chen, Y. J. *J. Phys. Chem. C* **2010**, *114*, 16229.
- [4] Hu, J. Q.; Bando, Y.; Zhan, J. H.; Golberg, D. *Appl. Phys. Lett.* **2004**, *85*, 3593.
- [5] Liu, B.; Zeng, H. C. *Small* **2005**, *1*, 566.
- [6] Cao, J.; Sun, J. Z.; Hong, J.; Li, H. Y.; Chen, H. Z.; Wang, M. *Adv. Mater.* **2004**, *16*, 84.
- [7] Sun, X. M.; Li, Y. D. *Angew. Chem., Int. Ed.* **2004**, *43*, 597.
- [8] Wang, Q. B.; Liu, Y.; Ke, Y. G.; Yan, H. *Angew. Chem., Int. Ed.* **2008**, *47*, 316.
- [9] Lyon, J. L.; Fleming, D. A.; Stone, M. B.; Schiffer, P.; Williams, M. E. *Nano Lett.* **2004**, *4*, 719.
- [10] Yang, P. P.; Quan, Z. W.; Hou, Z. Y.; Li, C. X.; Kang, X. J.; Cheng, Z. Y.; Lin, J. *Biomaterials* **2009**, *30*, 4786.
- [11] Zhang, M.; Wu, Y. P.; Feng, X. Z.; He, X. W.; Chen, L. X.; Zhang, Y. K. *J. Mater. Chem.* **2010**, *20*, 5835.
- [12] Liu, S. S.; Chen, H. M.; Lu, X. H.; Deng, C. H.; Zhang, X. M.; Yang, P. Y. *Angew. Chem., Int. Ed.* **2010**, *49*, 7557.
- [13] Won, Y. H.; Aboagye, D.; Jang, H. S.; Jitianu, A.; Stanciu, L. A. *J. Mater. Chem.* **2010**, *20*, 5030.
- [14] Li, Y.; Wu, J. S.; Qi, D. W.; Xu, X. Q.; Deng, C. H.; Yang, P. Y.; Zhuang, X. M. *Chem. Commun.* **2008**, 564.
- [15] Mondal, J.; Sen, T.; Bhaumik, A. *Dalton Trans.* **2012**, *41*, 6173.
- [16] Bagley, M. C.; Lubinu, M. C. *Top. Heterocycl. Chem.* **2006**, *31*.
- [17] Domling, A.; Ugi, I. *Angew. Chem., Int. Ed.* **2000**, *39*, 3168.
- [18] Simon, C.; Constantieux, T.; Rodriguez, J. *Eur. J. Org. Chem.* **2004**, 4957.
- [19] Erkkila, A.; Majander, I.; Pihko, P. M. *Chem. Rev.* **2007**, *107*, 5416.
- [20] Laschat, S.; Becheanu, A.; Bell, T.; Baro, A. *Synlett* **2005**, 2547.
- [21] Dirwald, F. Z. *Angew. Chem., Int. Ed.* **2003**, *42*, 1332.
- [22] Beak, P.; Anderson, D. R.; Curtis, M. D.; Laumer, J. M.; Pippel, D. J.; Weisenburger, G. A. *Acc. Chem. Res.* **2000**, *33*, 715.
- [23] Kryshnal, G. V.; Serebryakov, E. P. *Russ. Chem. Bull.* **1995**, *44*, 1785.
- [24] Beckwith, A. L. J. *Tetrahedron* **1981**, *37*, 3073.
- [25] Kappe, C. O. *Angew. Chem., Int. Ed.* **2004**, *43*, 6250.
- [26] Hayes, B. L. *Aldrichimica Acta* **2004**, *37*, 66.
- [27] Roberts, B. A.; Strauss, C. R. *Acc. Chem. Res.* **2005**, *38*, 653.
- [28] De La Hoz, A.; Diaz-Ortiz, A.; Moreno, A. *Chem. Soc. Rev.* **2005**, *34*, 164.
- [29] Bonrath, W.; Paz Schmidt, R. A. In *Advances in Organic Synthesis*, Ed.: Atta-ur-Rahman, Bentham Science, Oak Park, IL, **2005**, Chapter 3, p. 81.
- [30] Cravotto, G.; Cintas, P. J. *Chem. Soc. Rev.* **2006**, *35*, 180.
- [31] Mason, T. J. *Chem. Soc. Rev.* **1997**, *26*, 443.
- [32] Sadeghzadeh, S. M.; Nasser, M. A. *Catalysis Today* **2013**, *217*, 80.
- [33] Nasser, M. A.; Sadeghzadeh, S. M. *J. Iran Chem. Soc.* **2013**, *10*, 1047.
- [34] Nasser, M. A.; Sadeghzadeh, S. M. *J. Chem. Sci.* **2013**, *125*, 537.
- [35] Nasser, M. A.; Sadeghzadeh, S. M. *Monatsh. Chem.* **2013**, *144*, 1551.
- [36] Riano, S.; Fernandez, D.; Fadini, L. *Catal. Commun.* **2008**, *9*, 1282.
- [37] Zonouzi, A.; Biniaz, M.; Mirazadeh, R.; Talebi, M.; Ng, S. W. *Heterocycles* **2010**, *81*, 1271.

(Pan, B.; Fan, Y.)